Postprint of: Szpakowska M., Płocharska-Jankowska E., Otto B., New bulk liquid membrane oscillator composed of two coupled oscillators with diffusion-mediated physical coupling, CHEMICAL PAPERS, Vol. 69, Iss. 9 (2015), pp. 1176-1186

New bulk liquid membrane oscillator composed of two coupled oscillators with diffusion mediated physical coupling

Maria Szpakowska*, Elżbieta Płocharska-Jankowska, Ottó B. Nagy

Department of Quality Management and Commodity Science, Faculty of Management and Economics, Gdańsk University of Technology, 80-233 Gdańsk, ul. Narutowicza 11/12, Poland

Received 24 October 2014; Revised 12 January 2015; Accepted 3 February 2015

A new type of bulk liquid membrane system, which represents the first example of a bulk liquid membrane oscillator characterised by the presence of two coupled oscillators, is described. When the benzyldimethyltetradecylammonium chloride surfactant undergoes an oscillatory mass transfer through a nitromethane liquid membrane, a new liquid layer (phase X) appears between the membrane and the acceptor phase. Kinetic analysis provides evidence that the whole system is composed of two coupled oscillators with diffusion-mediated physical coupling. The first component oscillator (based on nitromethane) of lower frequency delivers the driving material to the second one (phase X-based oscillator) leading to additional higher frequency oscillations. A new molecular mechanism is proposed for interpreting the experimental observations. The results might enhance understanding of intercellular communication in biology, where periodic signalling is more efficient than any other type of signalling mode.

Keywords: phase separation, chemical kinetics, numerical simulations, coupled oscillations

*Corresponding authors, e-mail: mszpak@pg.gda.pl

Introduction

Non-linear oscillations accompanying mass transfer through liquid–liquid interfaces may play an important role in the engineering of micro-heterogeneous systems such as colloids and emulsions and in the processes taking place in biomembranes (Larter, 1990; Kovalchuk & Wollhardt, 2006). Liquid membrane systems are useful models for studying these highly complex systems thanks to their simplicity and versatility; they may also find applications in areas such as phase transfer catalysis, taste sensors, and in biological actions (Rastogi & Srivastawa, 2001).

The oscillatory character of the mass transfer across the liquid–liquid interfaces present in liquid membrane systems is shown by the periodic variation of some physicochemical property; this is known as a liquid membrane oscillator (see below).

Bulk liquid membrane oscillators are composed of two aqueous phases separated by an immiscible organic phase (membrane, m). One of the aqueous phases contains a surfactant, benzyldimethyltetradecylammonium chloride (BDMTACl), in the donor phase, d, while the other (acceptor phase, a) may or may not contain some kind of solute (e.g. sucrose). The organic phase contains appropriate substances (picric acid, HPi) for facilitating the transfer of the surfactant from the donor to the acceptor phase. The electric potential difference between the donor and acceptor phases exhibits oscillations when the mass transfer occurs in an oscillatory way (Szpakowska et al. 2002).

In order to contribute to elucidation of the molecular mechanism responsible for the observed oscillations, the physico-chemical properties of bulk liquid membrane oscillators with anionic (Szpakowska et al., 2008) and cationic (Szpakowska et al, 2002, 2003, 2006a, 2009) mass transfer surfactants and different membrane materials (Szpakowska et al., 2006a, 2006b, 2008, 2009) were investigated in detail. The influence of taste substances (Szpakowska et al., 2005, 2006a) was also examined and analysed in depth by the Gabor transformation (Płocharska-Jankowska et al., 2005, 2006).

The theoretical interpretation of the mechanism of these oscillations is based on two different approaches. In the hydrodynamic approach, it is the hydrodynamic instability of the liquid–liquid interfaces arising from the Marangoni effect which is responsible for the oscillations (Kovalchuk & Vollhardt, 2006). The corresponding mathematical analysis involves the solution of a set of non-linear, non-steady state Navier–Stokes equations and the surfactant diffusion equation. Notwithstanding the mathematical complexities, this approach leads to highly geometry-dependent results (Kovalchuk & Vollhardt, 2007). Hydrodynamic

arguments were also used in the case of biphasic systems to explain the observed periodic Marangoni instability (Lavabre et al., 2005; Ikezoe et al., 2004).

On the other hand, the chemical kinetic approach completely neglects the hydrodynamic aspects. It uses the laws of chemical kinetics based on autocatalytic reactions or cooperative adsorption of the transferring surfactant molecules at the liquid–liquid interfaces (Kovalchuk & Vollhardt, 2006; Yoshikawa et al., 1988; Yoshikawa & Matsubara, 1983; Toko et al., 1985; Pimienta et al., 2001). Some of the published models present inconsistencies. The working kinetic equations are not always in accord with the laws of chemical kinetics or they are based on unrealistic assumptions (Szpakowska et al., 2006b; Yoshikawa et al., 1988; Yoshikawa & Matsubara, 1983; Toko et al., 1985; Pimienta et al., 2001). This situation led to the proposal of a new sufficiently general and physicochemically acceptable mechanism for analysis by the chemical kinetics method of the bulk liquid membrane oscillations observed (Szpakowska et al., 2009).

In a previous publication (Szpakowska et al., 2009), the physicochemical properties of a nitrobenzene bulk liquid membrane oscillator containing BDMTACl surfactant in an aqueous donor phase were presented and a molecular mechanism was proposed using the chemical kinetic approach. It was shown that the actual oscillations of the electric potential difference between the two aqueous phases appeared at the liquid membrane–aqueous acceptor phase interface (m/a). They originated from the sudden autocatalytic adsorption and desorption of surfactant molecules at the m/a interface. The Marangoni effect also amplified the observed phenomenon (Kovalchuk & Vollhardt, 2006). These results clearly showed that the m/a interface played a decisive role in the appearance of oscillations. Accordingly, it appeared to be important to investigate how the properties of the liquid membrane could influence the characteristics of the oscillations. In particular, it was assumed that the quality of interface layer separating the membrane from the aqueous acceptor phase might have a decisive influence on the observed oscillations. This could be verified by setting up a liquid membrane oscillator containing a more water-soluble membrane material.

Nitromethane (NM) was seen to be a good candidate for this purpose. Its dielectric constant (35.87) is comparable with that of nitrobenzene (NB) (34.82) at T = 298.15 K (Reichardt, 1979) but its viscosity is much smaller (0.627 mPa·s for NM and 1.823 mPa·s for NB) (Weast et al., 1984). On the other hand, NM is much more soluble in water than NB: at T = 298.15 K, the dissolved organic solvent in water has a mole fraction of 35.33×10^{-3} for NM and 0.30×10^{-3} for NB (Marcus, 1977). Also, water dissolves better in NM than in NB: 0.0675 and 0.0162 in mole fractions, respectively (Marcus, 1977).

Unexpectedly, this NM-based bulk liquid membrane oscillator exhibited a completely new feature not observed in previous studies. During the transport process, a new liquid layer (phase X) appeared between the membrane and the acceptor phase. This kind of phase separation was previously observed in the case of a liquid membrane oscillator with anionic surfactant (Suzuki & Kawakubo, 1992). The authors interpreted the interfacial oscillations from the hydrodynamic perspective.

The appearance of the new X phase in the NM bulk liquid membrane oscillator containing hexadecyltrimethylammonium bromide (Szpakowska et al., 2006b) was also observed previously. However, the proposed mechanism could not satisfactorily account for the actual interconnection between the behaviour of the liquid membrane and the new phase.

An attempt was made to apply a mechanism proposed by Pimienta et al. (2001) to explain the oscillations of a dichloromethane-based bulk liquid membrane oscillator. According to these authors, the adsorption sites play a central role in the molecular events taking place at the water–membrane interfaces. This approach was appropriate for a strongly hydrophobic membrane but it did not afford satisfactory results when a much less hydrophobic membrane such as nitromethane is used since this latter is characterised by a less well-defined interface structure. Hence, a new mechanism is presented here, being a logical extension of the mechanism for the NB bulk liquid membrane oscillator previously considered (Szpakowska et al., 2009).

Furthermore, the oscillation patterns previously published did not exhibit a satisfactory regularity. It was hoped that, by changing the transferring surfactant molecule, more regular oscillation patterns might be obtained. Accordingly, it might be more appropriate for applications in taste recognition.

In the present paper, this new NM-based bulk liquid membrane oscillator containing BDMTACl is investigated and analysed using the chemical kinetic approach.

Experimental

The purification of chemicals, the experimental set-up and procedure were as published previously (Szpakowska et al., 2003). NM, like NB, has a greater density than water, hence the NM liquid membrane occupied the bottom of a U-shaped glass tube and the two branches contained the aqueous donor (d) and aqueous acceptor (a) phases (Fig. 1). At the beginning of the experiment, the electrodes were positioned at different distances from the

d/m and a/m interfaces. The following electrode distances were investigated: 1 cm – 1 cm, 1 cm – 2 cm, 2 cm – 1 cm, 2 cm – 2 cm, 3 cm – 3 cm, where the first number is the electrode distance from the d/m interface.

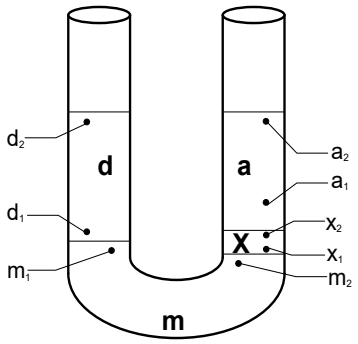

Fig. 1. Schematic view of experimental apparatus showing reference points used for measuring electric potential differences between the points i and j, $E_{i/j}$ (Eq. (1)), d – aqueous donor phase, m – membrane, a – aqueous acceptor phase.

The ambient temperature under which the experiments were performed varied between (18 ± 0.1) ºC and (28 ± 0.1) ºC. The surfactant concentration in the donor phase was changed from 2 mM to 10 mM, while the picric acid (HPi) concentration in the membrane phase was examined from 0 mM to 3 mM. The effect of membrane volume (from 6.0 cm^3 to 5.0 cm^3) on the oscillation pattern was also examined.

The actual optimised composition of the three phases was as follows:

m – 5.0 cm^3 of 1.5×10^{-3} M solution of HPi in NM;

d – 4.0 cm^3 of 5×10^{-3} M solution of BDMTACl in ethanol–water mixture (1.5 M);

a – 4.0 cm^3 of 0.1 M solution of sucrose in water.

In the case of the NM oscillator, the microelectrodes used for measuring the electric potential differences in the organic membrane phase (Eq. (2)) had to be modified in relation to the microelectrode applied in the NB oscillator. In particular, the internal solution of the electrode was composed of an 0.02 M solution of tetrabutylammonium chloride in nitromethane.

The oscillation curves were repeated at least four times for each case. The curves obtained were similar (difference in amplitude and frequency of peaks within 15 %). They were sensitive to the initial conditions, e.g. temperature, the manner of preparation of the interfaces.

The numerical integration of the differential equations was effected using the program Matlab R 12, ODE 45 with steps 0.01.

Results and discussion

Since the behaviour of liquid membrane oscillators is highly sensitive to the experimental parameters (electrode positions, temperature of measurements, membrane volume, initial concentrations of surfactant and HPi), these parameters had to be optimised.

Fig. 2 shows the influence of temperature on the oscillation pattern observed. This figure actually shows the time-dependence of the electric potential difference between the two aqueous phases, d and a, as measured at electrode positions d_1 and a_1 (see Fig. 1).

The oscillations are shown to be characterised by large low-frequency peaks flanked by lateral higher-frequency oscillations. The most satisfactory pattern was obtained at θ = (25 ± 0.1) ºC (Fig. 2c). It should be noted that this curve was previously used in molecular recognition studies (Szpakowska et al., 2005; Płocharska-Jankowska et al., 2005).

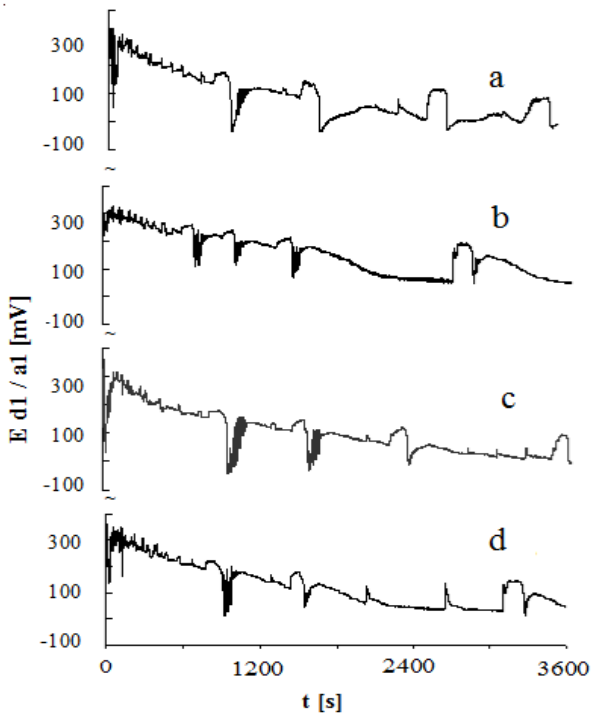

Fig. 2. Oscillation patterns of liquid membrane oscillator with NM at different temperatures θ/ºC: 18.0 ± 0.1 (a), 22.0 ± 0.1 (b), 25.0 ± 0.1 (c), and 28.0 ± 0.1 (d).

Fig. 3 shows the influence of electrode distances from the d/m interface and from the a/m interface on the oscillation pattern. The characteristic peaks are observed for the case when the electrodes were positioned at 2 cm from the interfaces in both the donor and acceptor phases (Fig. 3d).

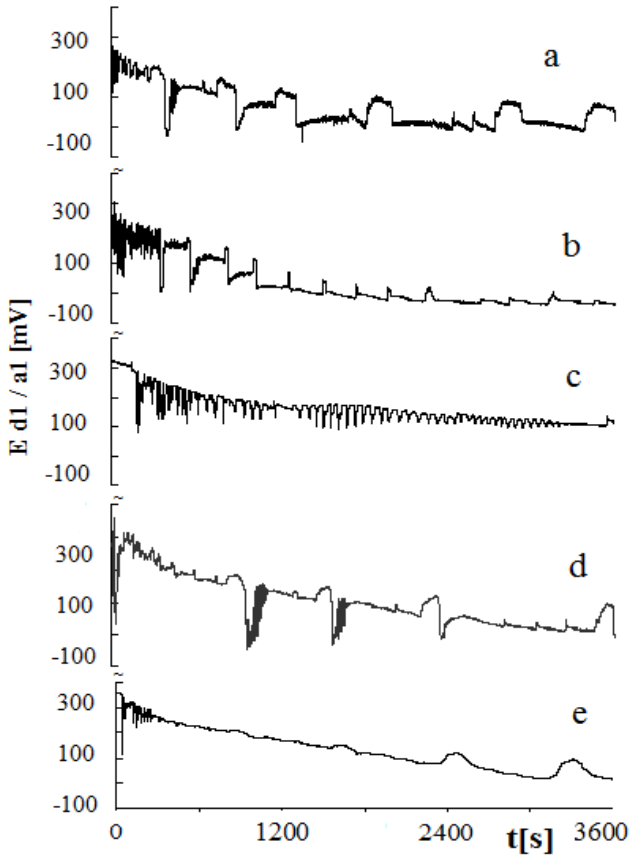

Fig. 3. Dependence of oscillation pattern of NM liquid membrane oscillator on initial electrode distances from d/m and a/m interfaces: 1 cm – 1 cm (a), 1 cm – 2 cm (b), 2 cm – 1 cm (c), 2 cm – 2 cm (d), 3 cm – 3 cm (e).

Fig. 4 indicates that too low and too high an initial concentration of surfactant in the donor phase does not produce oscillations. The most satisfactory oscillation pattern was found for the initial surfactant concentration of 5.0 mM (Fig. 4c).

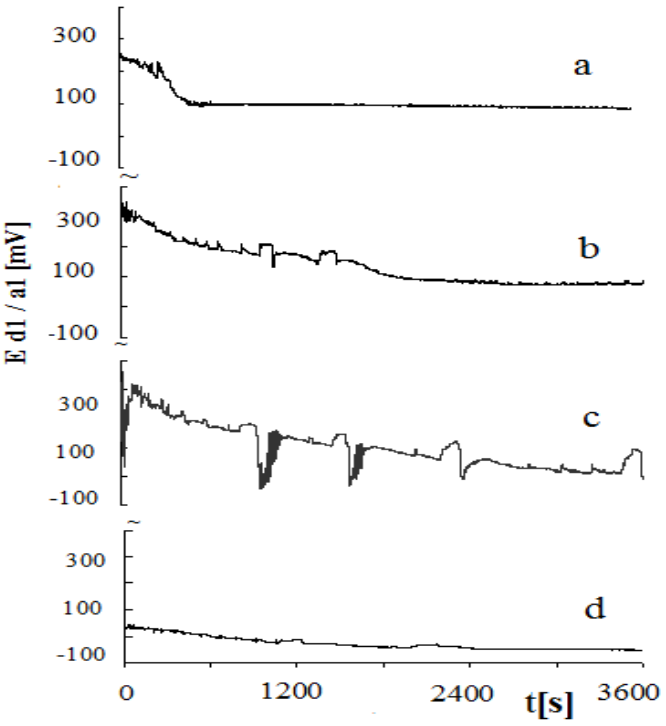

Fig. 4. Influence of initial surfactant concentration in donor phase on oscillation patterns of liquid membrane oscillator with NM: 2 mM (a), 3 mM (b), 5 mM (c), 10 mM (d); (θ = (25.0 ± 0.1) ºC).

The initial HPi concentration in the membrane phase also influences the $E_{d/a} = f(t)$ dependence (Fig. 5). The oscillation pattern is only observed at 1.5 mM initial HPi concentration in the membrane phase.

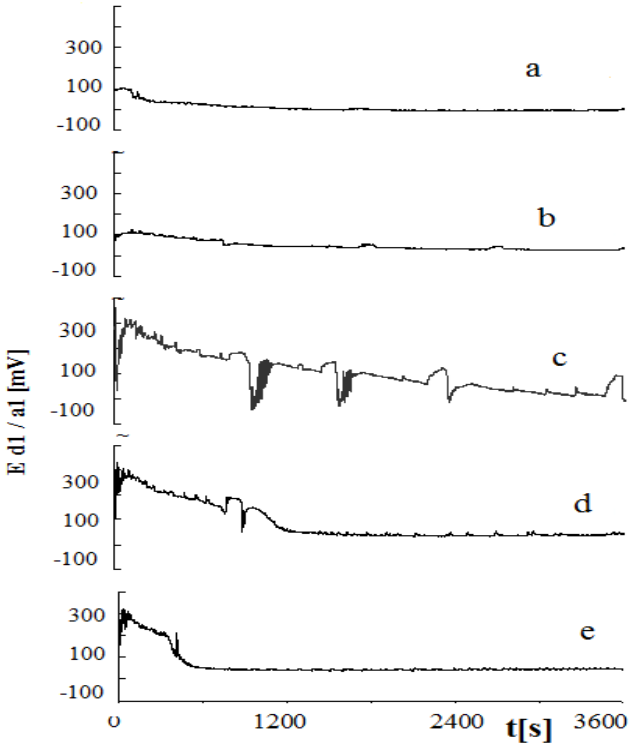

Fig. 5. Influence of initial HPi concentration in NM membrane phase on oscillation patterns: 0 mM (a), 0.75 mM (b), 1.5 mM (c), 2 mM (d), 3 mM (e); (θ = (25.0 ± 0.1) ºC).

The membrane volume also has an effect on the oscillation (Fig. 6). The 5.0 cm^3 volume appears to be optimal for observing the oscillations, hence was chosen for further experiments (Fig. 6c). Greater volumes increase the diffusion path between the donor and acceptor phases leading to oscillations, the beginning of which is delayed by several hours. At a membrane volume of 5.5 cm^3, this delay is around 2 h, while for a volume of 6.0 cm^3 the delay extends up to 5 h. Experiments with a membrane volume lower than 5.0 cm^3 could not be performed due to mutual leaking of the aqueous donor and acceptor phases.

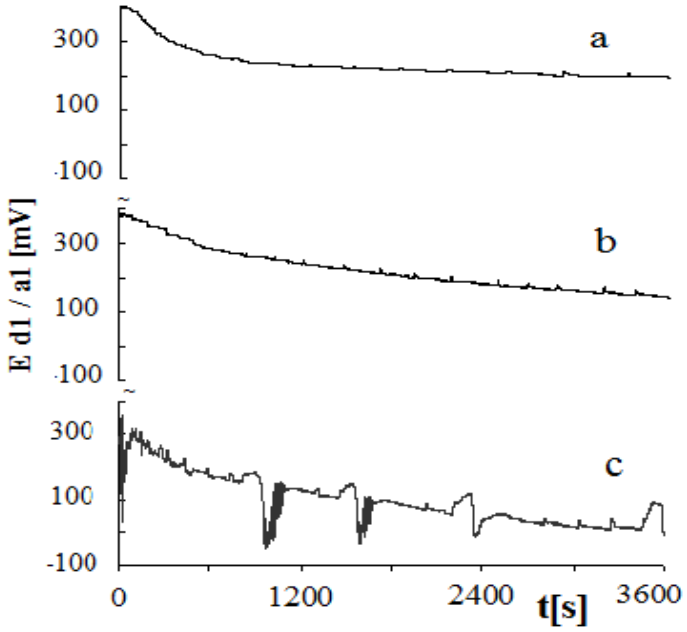

Fig. 6. Oscillation patterns of liquid membrane oscillator with NM at different liquid membrane volume: 6.0 mL (a), 5.5 mL (b), 5.0 mL (c); (θ = (25 ± 0.1) ºC).

The optimized values of the experimental parameters are detailed under Experimental; these were used in all the experiments. Although the experimental conditions were similar to those of the NB oscillator (Szpakowska et al., 2009), the behaviour of the oscillator under study proved to be completely different from previous observations. A spectacular new phenomenon appeared at about t = 300 s after the beginning of the experiment: a new separate layer denoted as phase X developed between the liquid membrane and the aqueous acceptor phase (Fig. 1).

Phase X was found to be an NM/water mixture, with its volume increasing over time. The intensive surface movements (Marangoni instability) observed visually at the m/a interface decreased considerably after t = 120 s and disappeared completely after t = 600 s. No surface movements were observed at the d/m interface. This confirmed that the oscillations in the electric potential difference between the two aqueous phases appeared at the m/a interface.

The physicochemical aspects of the liquid membrane oscillators were analysed in detail in a previous publication (Szpakowska et al., 2009). The overall electric potential

difference between the d and a aqueous phases, $E_{d/a}$, was shown to be the sum of different contributions. In considering the scheme in Fig. 1, it may be written as:

$$E_{d/a} = E_{d2/a2} = E_{d2/d1} + E_{d1/m1} + E_{m1/m2} + E_{m2/X1} + E_{X1/X2} + E_{X2/a1} + E_{a1/a2} \quad (1)$$

where: $E_{d2/d1}$, $E_{a1/a2}$, $E_{m1/m2}$ and $E_{X1/X2}$ are diffusion potentials in donor, acceptor, membrane and X phases, respectively. $E_{d1/m1}$, $E_{m2/X1}$ and $E_{X2/a1}$ are the potential differences across the donor phase/membrane, membrane/X phase and X phase/acceptor phase interfaces.

The diffusion potential differences in the two aqueous phases, $E_{d2/d1}$ and $E_{a1/a2}$, are ignored since their values are negligibly small (Szpakowska et al., 2003).

In principle, the different components in Eq. (1) can be measured experimentally by means of microelectrodes. However, this was impossible for the components involving phase X on account of the small volume of the latter. Accordingly, the last three components were combined, affording Eq. (2):

$$E_{d/a} = E_{d1/m1} + E_{m1/m2} - E_{a1/m2} \quad (2)$$

where $E_{m2/a1} = E_{m2/X1} + E_{X1/X2} + E_{X2/a1}$.

The results are collected in Table 1.

Table 1. Comparison of experimental and calculated (Eq. (2)) electric potential differences between the donor and acceptor phases, $E_{d/a}$, in function of time

Time, t	Potential difference/mV				
s	$E_{d1/m1}$	$E_{a1/m2}$	$E_{m1/m2}$	$E_{d/a}$ (calc)	$E_{d/a}$ (exp)
600	115	–130	25	270	265
1800	110	–100	5	215	230
2400	110	–60	0	170	180
3000	110	–50	0	160	165

It can be seen that $E_{d1/m1}$ essentially remains constant throughout the experiment. This indicates that the d/m interface is saturated with surfactant molecules. The diffusion potential in the membrane, $E_{m1/m2}$, only makes a small contribution. It is noteworthy that the calculated values of the overall electric potential difference, $E_{d/a}$ (calc), are in fairly good agreement with the directly measured values, $E_{d/a}$ (exp). This confirms the validity of Eq. (2) throughout the experiment.

According to theory (Suzuki & Kawakubo, 1992; Sternling & Scriven, 1959; Brian, 1971), the Marangoni effect observed in the initial stage of the experiments depends on the relative magnitudes of the kinematic viscosities (η_i) of the two phases in contact and of the solute diffusion coefficients (D_i) in the two phases, as well as on the direction of the solute transfer gradient and the sign of change in interfacial tension with solute concentration. When a surfactant is transferred from phase A to phase B, and if $\eta_A/\eta_B > 1$ and $D_A/D_B < 1$, a large Marangoni effect can be expected. With A = nitrobenzene and B = water, these conditions were fulfilled at the m/a interface and a significant Marangoni effect was observed (Szpakowska et al., 2009). On the other hand, if $\eta_A/\eta_B < 1$ and $D_A/D_B > 1$, the interface remains stable and the Marangoni effect is absent. This pertained for the d/m interface with NB membrane.

In the present case, the kinematic viscosity of NM is smaller (0.554×10^{-6} m^2 s^{-1}) (Weast et al., 1984) than that of water (w) (0.891×10^{-6} m^2 s^{-1}) (Weast et al., 1984), i.e. $\eta_{NM}/\eta_w < 1$. With $D_i \sim \eta_i^{-1}$, there is $D_{NM}/D_w > 1$ and no Marangoni effect, which originates from the solute transfer gradient, could be detected at the m/a interface.

The significant Marangoni effect observed experimentally at the m/a interface conflicts with this theoretical prediction based on solute transfer gradients (Sternling & Scriven, 1959). However, a more precise theory based on linear stability analysis predicts that an interface is always unstable under the conditions of surfactant transfer if the adsorption kinetics is diffusion-controlled (Hennenberg et al. 1979).

Another explanation may be presented for the effects observed in the present case. It is well known that the interpenetration of two liquids (e.g. water and nitromethane) under non-equilibrium conditions may provoke a dynamic interfacial tension gradient which can lead to large Marangoni effects (Ostrovsky & Ostrovsky, 1983). The increased mutual solubility of NM and water induces a much greater interface instability than in the case of NB. The Marangoni effect disappears after $t = 600$ s (see above) when the interpenetration of the two phases stops at the equilibrium state determined by the mutual solubility.

The oscillatory behaviour of the overall electric potential difference between the aqueous donor and acceptor phases, $E_{d/a}$, at the actual optimized initial composition of the three phases is represented in Fig. 2c (and also in Figs 3d, 4c, 5c and 6c).

It can be seen that the oscillation pattern observed is quite different from that of the NB oscillator. This latter had regular, high-frequency oscillations with apparently constant amplitudes throughout the experimental run. On the other hand, the NM oscillator may be characterised by the presence of much larger peaks of smaller amplitudes. These peaks appear after a long induction period and after the vanishing of high-frequency irregular transient oscillations.

An important new feature of the NM oscillator is that the large peaks are accompanied on their right by much higher frequency oscillations. This contrasts with the rather long periods observed for the large peaks.

Kinetics and mechanism

In order to obtain greater insight into the molecular events taking place in the oscillator at hand, the same chemical approach is applied as for the NB oscillator using the laws of chemical kinetics (Szpakowska et al., 2009). In this approach, a given molecule is considered as a different species if situated in different environments. It is further admitted that the transformation of one species into another is governed by the laws of deterministic chemical kinetics.

The ion pair mechanism previously proposed is adopted and modified to take into account the presence of the new phase X. The various mechanistic steps are represented in Fig. 7.

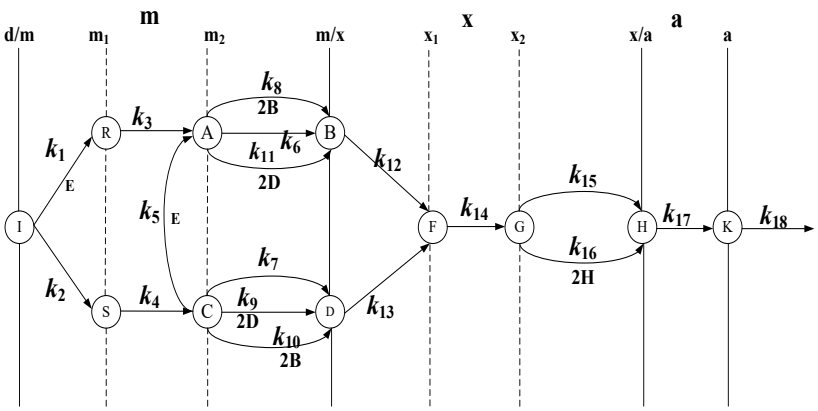

Fig. 7. Mechanistic scheme of NM-based oscillator.

The interface d/m is saturated with surfactant I which desorbs to vicinity m_1 of the interface in the NM membrane in the form of ion pairs with counter ions Cl^- (S) and Pi^- (R), where E denotes HPi and k_1 and k_2 are appropriate rate constants.

The tendency of the surfactant to penetrate into the membrane from the donor phase is indicated by the large value of its partition constant: $K_m/K_d = 45 \pm 1$ at (25 ± 0.1) °C.

The ion pairs R and S diffuse through the membrane to vicinity m_2 of the m/X interface (rate constants k_3 and k_4). Ion pairs C may react with HPi to form the other type of ion pairs A (k_5).

The ion pairs at m_2, A, and C, suddenly adsorb into the m/X interface in non-catalysed (rate constants k_6 and k_7) and catalysed steps (rate constants k_8 and k_9). Clearly, cross-catalytic steps may also occur (rate constants k_{10} and k_{11}). Due to these adsorption steps, interface m/X becomes positively charged and the electric potential difference, $E_{d/a}$, suddenly decreases to a smaller value.

In subsequent steps, ion pairs B and D are desorbed to vicinity X_1 of the m/X interface in phase X (rate constants k_{12} and k_{13}). It is assumed that, in phase X, both ion pairs are completely dissociated due to the high dielectric constant of water present. Hence, both ion pairs give the same cationic species F.

The desorbed surfactant diffuses across phase X to vicinity X_2 of the X/a interface, giving G (k_{14}). Desorption (k_{12} and k_{13}) eliminates the positive charge from interface m/X and $E_{d/a}$ regains a value which is close to its original value.

Once more, the surfactant ion is suddenly adsorbed to the X/a interface in non-catalysed (k_{15}) and catalysed steps giving H (k_{16}). As a result, these adsorption steps decrease the value of $E_{d/a}$.

Finally, the surfactant is suddenly desorbed to vicinity a_1 of the X/a interface (k_{17}), followed by the diffusion of the desorbed surfactant K from a_1 into the bulk of the acceptor phase, a_2 (k_{18}). The desorption step again provokes the increase in $E_{d/a}$ value.

Repetition of the adsorption–desorption steps leads to oscillation of the electric potential difference $E_{d/a}$. The oscillations observed are seen as due to the mass transfer of surfactant from the aqueous donor to the aqueous acceptor phase in an oscillatory way (Szpakowska et al., 2009). Spectrophotometric measurements revealed that, for the initial

surfactant concentration of $I_0 = 5.0 \times 10^{-3}$ M in the donor phase, the values of 5.0×10^{-6} M were found after t = 3600 s in the acceptor phase. At the same time, the counter ion concentration dropped to $[Cl^-] = 4.1 \times 10^{-4}$ M in the acceptor phase. The difference is due to the different partitioning of the surfactant and its counter ion in the membrane and in phase X.

The presence of surfactant in the acceptor phase was also confirmed by NMR measurements. HPi is also transferred to the acceptor phase. Its concentration was 6.0×10^{-5} M after t = 3600 s, as revealed by UV spectroscopy. Again, the NMR results confirmed the presence of HPi in the acceptor phase. On the other hand, no HPi was detected in the donor phase.

The time evolution of the molecular events participating in the oscillation process can be described by the corresponding chemical kinetics equations (for simplicity, the charges are not represented in these equations). Only the forward reaction steps are considered (far from equilibrium situation) and the hydrodynamic effects are not taken into account explicitly.

The proposed mechanistic scheme (Fig. 7) shows that its first part (steps $k_1 - k_{14}$) is identical with the scheme applied to the nitrobenzene-based oscillator previously published (Szpakowska et al., 2009). The second part is due to the presence of phase X.

The following rate equations can be established for the proposed mechanism:

$$dR/dt = k_1IE - k_3R \quad (3)$$

$$dS/dt = k_2I - k_4S \quad (4)$$

$$dA/dt = k_3R + k_5EC - k_6A - k_8AB^2 - k_{11}AD^2 \quad (5)$$

$$dB/dt = k_6A + k_8AB^2 + k_{11}AD^2 - k_{12}B \quad (6)$$

$$dC/dt = k_4S - k_5EC - k_7C - k_9CD^2 - k_{10}CB^2 \quad (7)$$

$$dD/dt = k_7C + k_9CD^2 + k_{10}CB^2 - k_{13}D \quad (8)$$

$$dF/dt = k_{12}B + k_{13}D - k_{14}F \quad (9)$$

$$dG/dt = k_{14}F - k_{15}G - k_{16}GH^2 \quad (10)$$

$$dH/dt = k_{15}G + k_{16}GH^2 - k_{17}H \quad (11)$$

$$dK/dt = k_{17}H - k_{18}K \quad (12)$$

Eqs. (3)–(12) represent a system of autonomous first-order coupled non-linear differential equations in as much as time does not appear explicitly (however, see below). The solution of this system was obtained by numerical integration using the Matlab program.

The actual values of the different rate constants k_i were chosen according to the physical chemistry of the system (Szpakowska et al., 2009). By analogy, k_3 and k_4 represent

normal diffusion steps. Hence, their values might be around 10^{-5} as suggested by data in the literature (Cussler, 1995). As in a previous publication (Szpakowska et al., 2009), these values were taken only as indications for diffusion steps k_3 and k_4. They were used as the starting point for further numerical experimentation but other values might also have been used. There is also $k_3 < k_4$ due to the size difference of the diffusing species. On the other hand, the diffusion step in phase X is characterised by the rate constant k_{14} which represents super-diffusion (i.e. diffusion promoted by the Marangoni effect), hence its value must be much higher than that of k_3 and k_4. A further contribution to the higher value of k_{14} derives from the fact that the new phase X is much thinner than the liquid membrane.

The experiment reveals that the thickness of phase X increases over time. This means that diffusion across phase X becomes more and more retarded as the diffusion path increases. As a result, the value of k_{14} must decrease with time. The time-dependence of k_{14} could be expressed by the equation $k_{14} = \alpha/(1 + \beta t)$, where α and β are the appropriately chosen constants and t represents the time. It should be noted that, by introducing an explicitly time-dependent rate constant, the system of differential equations becomes non-autonomous. For obvious reasons, the catalytic (k_8, k_9, k_{16}) and cross-catalytic (k_{10}, k_{11}) adsorption rate constants must have much greater values than the non-catalysed rate constants (k_6, k_7, k_{15}). Furthermore, sustained oscillations can be obtained only if the Gray–Scott condition (Szpakowska et al., 2009; Gray & Scott, 1990) is fulfilled: the desorption rate constants (k_{12}, k_{13}, k_{17}) must be substantially greater than the non-catalysed adsorption rate constants (k_6, k_7, k_{15}) at the m/X and X/a interfaces. More precisely, the following relationships must be satisfied: $k_{12} > 8k_6$, $k_{13} > 8k_7$ and $k_{17} > 8k_{15}$. Clearly, many different k_i values can satisfy these conditions.

In the present work, the following set of rate constants was used for model calculations: $k_1 = 2.5 \times 10^3$ M^{-1} s^{-1}; $k_2 = 2$ s^{-1}; $k_3 = 9 \times 10^{-6}$ s^{-1}; $k_4 = 10^{-5}$ s^{-1}; $k_5 = 1$ M^{-1} s^{-1}; $k_6 = 10^{-4}$ s^{-1}; $k_7 = 5 \times 10^{-4}$ s^{-1}; $k_8 = 10^5$ M^{-2} s^{-1}; $k_9 = 8 \times 10^4$ M^{-2} s^{-1}; $k_{10} = 9 \times 10^{-2}$ M^{-2} s^{-1}; $k_{11} = 10^{-1}$ M^{-2} s^{-1}; $k_{12} = 1.8$ s^{-1}; $k_{13} = 2.7$ s^{-1}; $k_{14} = 0.02/(1 + 5 \times 10^{-4}t)$s^{-1}, $k_{15} = 3 \times 10^{-3}$ s^{-1}, $k_{16} = 10^6$ M^{-2} s^{-1}, $k_{17} = 1.2$ s^{-1}, $k_{18} = 0.08$ s^{-1}.

With these k_i values and constant initial concentrations, $I_0 = 5.0 \times 10^{-3}$ M and $E_0 = 1.5 \times 10^{-3}$ M (the initial concentrations of all the other species were zero), numerical integration gave the oscillation curve (time series) represented in Fig. 8.

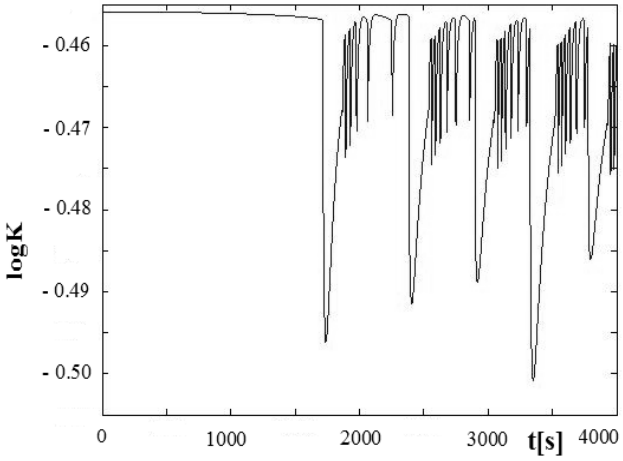

Fig. 8. Calculated oscillation profile of surfactant concentration, K, in aqueous acceptor phase (arbitrary scale).

It can be seen that the theoretical curve appropriately reflects the general characteristics of the experimental oscillation profile (Fig. 2c). Oscillations appear only after an induction period. The oscillation peaks are large, have low frequency and on their right they are accompanied by higher frequency oscillations with narrower peaks of lower amplitudes.

The proposed model can also be used for establishing the origin of the two types of oscillations present in the oscillation pattern. The presence of the new phase X suggests that the NM oscillator can be regarded as composed of two subsystems: the first is an oscillator having NM as membrane (m-oscillator) while the membrane of the second oscillator is the new phase X, i.e. a NM–water mixture (X-oscillator). It is quite probable that these two oscillators produce different oscillations. It is anticipated that, if the oscillations of one of these oscillators are suppressed, the oscillations of the other oscillator can be observed separately. A given oscillation can be readily blocked if the Gray–Scott condition (Gray & Scott, 1990) is not fulfilled. This occurs for an appropriate selection of the desorption and non-catalysed adsorption rate constants at the membrane exit interface (Szpakowska et al., 2009).

For example, if the inequality characterising the X-oscillator is reversed, i.e. if $k_{17} < 8k_{15}$, the corresponding stationary state cannot lose its stability and sustained oscillations are impossible. This pertains, for example, for the following choice of rate constants: $k_{15} = 3\ s^{-1}$ and the previous $k_{17} = 1.2\ s^{-1}$. The values of the other rate constants remained as for the curve presented in Fig. 8.

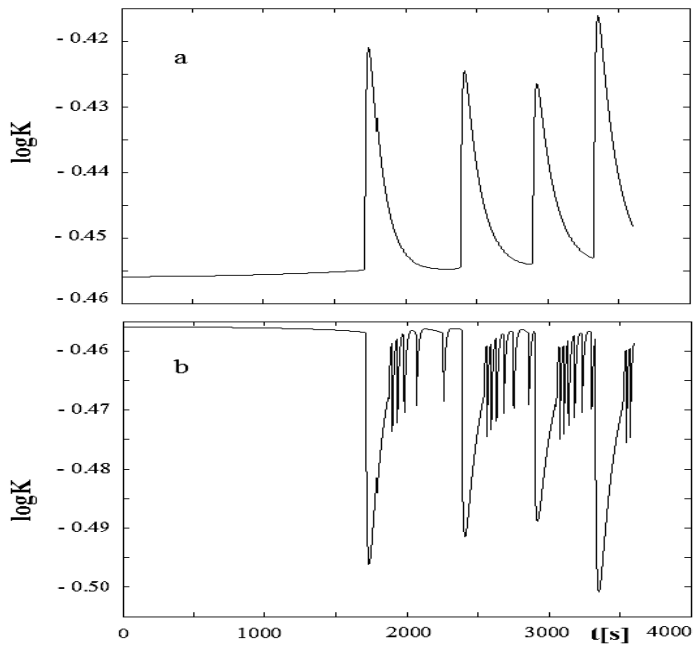

Fig. 9. Selective suppression of oscillations taking place in phase X; $k_{17} < 8k_{15}$ (a); $k_{17} > 8k_{15}$ (b).

Fig. 9 shows that the narrow small-amplitude higher-frequency peaks disappear from the right of the wide lower-frequency peaks. It may be concluded that the suppressed peaks originate from the oscillations taking place in the X-oscillator at the X/a interface. On the other hand, the remaining wide peaks represent the oscillations in the m-oscillator at the m/X interface. This is confirmed by the oscillation curve in Fig. 9a being identical with the oscillation pattern of species F.

The two component oscillators are coupled so that the first m-oscillator delivers the starting amount of surfactant to the second X-oscillator in an oscillatory manner; hence chemical-coupling in series (Epstein & Pojman, 1998). These oscillations of the first oscillator are modulated subsequently by the oscillations occurring in the second oscillator. Consequently, the experimental oscillation profile exhibits contributions from both parts of the investigated oscillator: one cycle of the m-oscillator is followed by several cycles of the X-oscillator. This complex oscillation pattern could be the result of a bursting mechanism or some kind of intermittency (Epstein & Pojman, 1998) observed for certain single oscillators. However, these possibilities can be excluded in the light of the above analysis.

The chemical coupling between the m- and X-oscillators is only formal since no actual chemical reactions take place in the system. The coupling between the two component

oscillators is physical, being based on the diffusion of species F from the m/X interface area (m-oscillator) to the X/a interface area. This can be shown by examining the role played by the diffusion rate constant, k_{14}, in the oscillation mechanism. When k_{14} increases (increasing constant α for a given value of β), the oscillations due to the m-oscillator (large peaks) remain almost unchanged: the amplitudes show little variation while the number of peaks and the periods are the same. However, the number of small narrow peaks (X-oscillator) and their amplitudes decrease considerably.

When k_{14} is decreased by increasing constant β for a given value of α, the characteristics of the large peaks again remain unchanged. On the other hand, the number of narrow peaks and their amplitudes increases and the oscillation in the X-oscillator begins later and later. When the narrow peaks reach the same amplitude as the large peaks, these latter become completely hidden and their presence is more and more difficult to detect. At a sufficiently high value of the constant β, no traces of the large peaks are visible and the oscillation pattern of the oscillator undergoes a transition to pure X-oscillations.

These results can be interpreted as follows: when k_{14} is high, the diffusion connecting the m- and X-oscillators is fast and the coupling is strong. The amount of F appearing near interface m/X in an oscillatory fashion is quickly delivered to vicinity x_2 of interface X/a. Oscillations at this interface start for each cycle of the appearance of the surfactant (species F) and both m- and X-oscillations appear in the oscillation pattern. On the other hand, the low k_{14} value means slower diffusion. As a consequence, more F accumulates near interface m/X and it has time to lose its oscillatory character before it is delivered slowly to the vicinity of the X/a interface. This means that, when k_{14} has a low value, the coupling between the m- and X-oscillators is weak and ultimately only the X-oscillations can be observed. It should be noted that the same result can be obtained by blocking the m-oscillator by choosing appropriate adsorption and desorption rate constants (see above). These results show that a strong physical coupling occurs in the NM liquid membrane oscillator.

For completeness, the chemical coupling present in the m-oscillator should also be mentioned. The coupling occurs between the oscillations of the two types of ion pairs, A and C, due to the presence of cross-catalytic steps (k_{10} and k_{11}). The strength of this chemical coupling is controlled by the corresponding rate constants, k_{10} and k_{11}, as shown in a previous publication (Szpakowska et al., 2009). In the present case also, k_{11} has a greater influence than k_{10} on the oscillation pattern. The systematic variation in both k_{10} and k_{11} shows that the actual experimental oscillation profile corresponds to weak chemical coupling.

This detailed analysis reveals that the kinetic approach previously proposed (Szpakowska et al., 2009) can also be used successfully in the case of more complex coupled oscillators.

The NM-based oscillator containing BDMTACl investigated in this work represents the second example of a liquid membrane oscillator showing phase separation and analysed by the chemical kinetics approach. In the first example, hexadecyltrimethylammonium bromide (HTMABr) was used as the transferring molecule. The oscillation patterns were different and less regular than in the present case. This indicates the high sensitivity of liquid membrane oscillators to their actual composition. This property can be successfully exploited in taste recognition. The mathematical description of the first case also involved the interphase structure but it did not lead to a wholly satisfactory description of the observed oscillation. In the present work, the mathematical description avoids considering the interphase structure and relies exclusively on chemical kinetics. This approach affords a highly satisfactory interpretation of the observed oscillations. Furthermore, it provides evidence for the coupling of the two component oscillators. It transpired that the new phase X which appeared between the liquid membrane and the aqueous acceptor phase was the site of a second oscillator. The strong coupling of this latter to the basic oscillator of the system is responsible for the complex oscillatory behaviour. The importance of phase separation is clearly indicated, hence its presence should be carefully investigated in each case prior to any interpretation of the experimental results being attempted.

Conclusions

The present work clearly demonstrates that, when the characteristics of the liquid-liquid interfaces present in a liquid membrane oscillator are modified, somewhat unpredicted results can be obtained.

More specifically, when a more “water-soluble” solvent, nitromethane, is used as a membrane in the liquid membrane oscillator, a wholly new oscillatory behaviour is observed. First of all, the rapid interpenetration of the two liquids in contact, water and nitromethane, produces a powerful Marangoni effect. Unexpectedly, a new phase X is formed between the membrane and the aqueous acceptor phase. The oscillator profile corresponds to a new type of oscillation system. Unusually large and small amplitude peaks are accompanied by several narrower peaks of higher frequency. It was shown that these high-frequency peaks are due to

oscillations taking place in phase X at the X/a interface (X-oscillator). On the other hand, the large peaks represent oscillations taking place at the m/X interface (m-oscillator). Their unusual width probably stems from the fact that the interface layer separating two liquids having partial mutual solubility is considerably larger than in the case of only slightly soluble liquids such as water and nitrobenzene.

The NM-based oscillator investigated in the present work is actually composed of two component oscillators which are coupled in series by physical coupling. The final state of the transferring surfactant F in the m-oscillator is the starting material for the X-oscillator. The degree of coupling is controlled by diffusion of the surfactant from the vicinity of the m/X interface to the proximity of the X/a interface. The proposed mechanistic scheme implies a formal chemical coupling also between the two kinds of ion pairs present in the m-oscillator (cross-catalytic steps).

By applying the laws of chemical kinetics to the proposed mechanistic steps, the time-evolution of the concentrations of all the species present could be obtained by numerical integration of the kinetic equations. The results accord relatively well with the general features of the experimental oscillation profile. Analysis shows that the physical coupling is rather strong while the chemical coupling is relatively weak. In agreement with previous results (Szpakowska et al., 2009), the present study also shows that the chemical kinetic approach is quite versatile and can be successfully used for unravelling mechanistic details even in the case of coupled liquid membrane oscillators. Accordingly, the results obtained here might contribute to a better understanding of intercellular communication in biology where the periodic signalling is more efficient than any other type of signalling mode (Goldbeter, 1996).

Finally, it should be stressed that the present work provides evidence for the coupling in a spontaneously created coupled oscillator as opposed to artificially constructed oscillatory systems (Tatsuno et al., 2012).

References

Brian, P. L. T. (1971). Effect of Gibbs adsorption on Marangoni instability. *AIChE Journal*, *17*, 765–772. DOI: 10.1002/aic.690170403.

Cussler, E. L. (1995). *Diffusion: Mass transfer in fluid systems*. Cambridge: UK: Cambridge University Press.

602 Epstein, I. R., & Pojman, J. A. (1998). *An introduction to nonlinear chemical dynamics*. New
603 York, NY, USA: Oxford University Press.
604 Goldbeter, A. (1996). *Biochemical oscillations and cellular rhythms*. Cambridge: UK:
605 Cambridge University Press.
606 Gray, P., & Scott, S. K. (1990). *Chemical oscillations and instabilities: Non-linear chemical*
607 *kinetics*. New York, NY, USA: Oxford University Press.
608 Hennenberg, M., Bisch, P. M., Vignes-Adler, M., & Sanfeld, A. (1979). Mass transfer,
609 Marangoni effect, and instability of interfacial longitudinal waves: I. Diffusional exchanges.
610 *Journal of Colloid and Interface Science*, *69*, 128–137. DOI: 10.1016/0021-9797(79)90087-
611 0.
612 Ikezoe, Y., Ishizaki, S., Yui, H., Fujinami, M., & Sawada, T. (2004). Direct observation of
613 chemical oscillation at a water/nitrobenzene interface with a sodium-alkyl-sulfate system.
614 *Analytical Sciences*, *20*, 435–440. DOI: 10.2116/analsci.20.435.
615 Kovalchuk, N. M., &Vollhardt, D. (2006). Marangoni instability and spontaneous non-linear
616 oscillations produced at liquid interfaces by surfactant transfer. *Advances in Colloid*
617 *Interface Science*, *120*, 1–31. DOI: 10.1016/j.cis.2006.01.001.
618 Kovalchuk, N. M., & Vollhardt, D. (2007). Instability and spontaneous oscillations by
619 surfactant transfer through a liquid membrane. *Colloids and Surfaces A: Physicochemical*
620 *Engineers Aspects*, *309*, 231–239. DOI: 10.1016/j.colsurfa.2006.11.040.
621 Larter, R. (1990). Oscillations and spatial nonuniformities in membranes. *Chemical Reviews*,
622 *90*, 355–381. DOI: 10.1021/cr00100a002.
623 Lavabre, D., Pradines, V., Micheau, J. C., & Pimienta, V. (2005). Periodic Marangoni
624 instability in surfactant (CTAB) liquid/liquid mass transfer. *The Journal of Physical*
625 *Chemistry B*, *109*, 7582–7586. DOI: 10.1021/jp045197m.
626 Marcus, Y. (1977). *Introduction to liquid state chemistry*. London, UK: Wiley.
627 Ostrovsky, M. V., & Ostrovsky, M. J. (1983). Dynamic interfacial tension in binary systems
628 and spontaneous pulsation of individual drops by their dissolution. *Journal of Colloid and*
629 *Interface Science*, *93*, 392–401. DOI: 10.1016/0021-9797(83)90422-8.
630 Pimienta, V., Etchenique, R., & Buhse, T., (2001). On the origin of electrochemical
631 oscillations in the picric acid/CTAB two-phase system. *The Journal of Physical Chemistry*
632 *A*, *105*, 10037–10044. DOI: 10.1021/jp013350w.
633 Płocharska-Jankowska, E., Szpakowska, M., Mátéfi-Tempfli, S., & Nagy, O. B. (2005). On
634 the possibility of molecular recognition of taste substances studied by Gábor analysis of
635 oscillations. *Biophysical Chemistry*, *114*, 85–93. DOI: 10.1016/j.bpc.2004.10.004.

Płocharska-Jankowska,E., Szpakowska, M., Matefi-Tempfli, S. & B.Nagy, O. (2006). A new approach to the spectra analysis of liquid membrane oscillators by Gabor transformation. *Journal of Physical Chemistry B,* 110, 289-294. DOI: 10.1021/jp0557870

Rastogi, R. P., & Srivastava, R. C., (2001). Interface-mediated oscillatory phenomena. *Advances in Colloid and Interface Science*, *93*, 1–75. DOI: 10.1016/s0001-8686(00)00037-3.

Reichardt, C. (1979). *Solvent effects in organic chemistry*. Weinheim, Germany: Verlag Chemie.

Sternling, C. V., & Scriven, L. E. (1959). Interfacial turbulence: Hydrodynamic instability and Marangoni effect. *AIChE Journal*, *5*, 514–520. DOI: 10.1002/aic.690050421.

Suzuki, T., & Kawakubo, T. (1992). Convective instability and electric potential oscillation in a water-oil-water system. *Biophysical Chemistry*, *45*, 153–159. DOI: 10.1016/0301-4622(92)87007-6.

Szpakowska, M., Czaplicka, I., Szwacki, J., & Nagy, O. B. (2002). Oscillatory phenomena in systems with bulk liquid membranes. *Chemical Papers*, *56*, 20–23.

Szpakowska, M., Czaplicka, I., Płocharska–Jankowska, E., & Nagy, O. B. (2003). Contribution to the mechanism of liquid membrane oscillators involving cationic surfactant. *Journal of Colloid and Interface Science*, *261*, 451–455. DOI: 10.1016/s0021-9797(03)00080-8.

Szpakowska, M., Płocharska-Jankowska, E., & Nagy, O. B. (2005). On the new possibility of applying oscillating liquid membrane systems for molecular recognition substances responsible for taste. *Desalination*, *173*, 61–67. DOI: 10.1016/j.desal.2004.06.209.

Szpakowska, M., Magnuszewska, A., & Płocharska-Jankowska, E. (2006a). Possibility of discrimination of sour substances by liquid membrane oscillators. *Desalination*, *198*, 353–359. DOI: 10.1016/j.desal.2006.04.003.

Szpakowska, M., Czaplicka, I., & Nagy, O. B. (2006b). Mechanism of four-phase liquid membrane oscillator containing hexadecyltrimethylammonium bromide. *The Journal of Physical Chemistry A*, *110*, 7286–7292. DOI: 10.1021/jp057349z.

Szpakowska, M., Magnuszewska, A., & Nagy, O. B. (2008). Mechanism of nitromethane liquid membrane oscillator containing sodium oleate. *Journal of Colloid and Interface Science*, *325*, 494–499. DOI: 10.1016/j.jcis.2008.05.059.

Szpakowska, M., Płocharska-Jankowska, E., & Nagy, O. B. (2009). Molecular mechanism and chemical kinetic description of nitrobenzene liquid membrane oscillator containing

669 benzyldimethyltetradecylammonium chloride surfactant. *The Journal of Physical Chemistry*
670 *B*, *113*, 15503–15512. DOI: 10.1021/jp9066873.
671 Tatsuno, Y., Kozuru, T., Yoshida, Y., & Maeda, K. (2012). Propagation and synchronization
672 of potential oscillations in multiple liquid membrane systems. *Analytical Science*, *28*, 1145–
673 1151. DOI: 10.2116/analsci.28.1145.
674 Toko, K., Yoshikawa, K., Tsukiji, M., Nosaka, M., & Yamafuji, K. (1985). On the oscillatory
675 phenomenon in an oil/water interface. *Biophysical Chemistry*, *22*, 151–158. DOI:
676 10.1016/0301-4622(85)80037-5.
677 Weast, R. C., Astle, M. J., & Beyer, W. H. (1984). *CRC handbook of chemistry and physics*
678 (64th ed.). Boca Ration, FL, USA: CRC Press.
679 Yoshikawa, K., & Matsubara, Y. (1983). Spontaneous oscillation of pH and electric potential
680 in an oil–water system. *Journal of the American Chemical Society*, *105*, 5967–5969. DOI:
681 10.1021/ja00357a001.
682 Yoshikawa, K., Shoji, M., Nakata, S., Maeda, S., & Kawakami, H. (1988). An excitable
683 liquid membrane possibly mimicking the sensing mechanism of taste. *Langmuir*, *4*, 759–
684 762. DOI: 10.1021/la00081a046.